BUFFET CONTROL BY MEANS OF MECHANICAL AND FLUIDIC VORTEX GENERATORS

J. DANDOIS[1], V. BRUNET[1], P. MOLTON[2], J.-C. ABART[2] and A. LEPAGE[3]
[1]*ONERA, Applied Aerodynamics Department, 8 rue des Vertugadins 92190 MEUDON*
[2]*ONERA, Fundamental and Experimental Aerodynamics Department, 8 rue des Vertugadins 92190 MEUDON*
[3]*ONERA, Aeroelasticity and Structural Department, 29 avenue de la Division Leclerc 92322 CHATILLON*

Summary

In the framework of the ONERA's internal research project BUFET'N Co, numerical simulations have been performed to help to the actuator parameters choice (actuator position, orifice diameter, pitch and skew angles…) and to the design of the wing model's inserts which have been tested in the ONERA S3Ch wind tunnel. Three-dimensional RANS computations have been realized to study both passive (mechanical VGs) and active (fluidic VGs) actuators. Concerning the mechanical VGs, three parameters have been studied: the skew angle, the spanwise spacing and the chordwise position. The effect of those three parameters on the lift, the wall pressure distribution has been investigated to determine the optimal parameters. Concerning the fluidic VGs, two parameters have been studied: the pitch and skew angles. Then, wind tunnel tests have been performed on a half-model in transonic conditions in the ONERA S3Ch wind tunnel. Experimental results have shown that both mechanical and fluidic VGs were effective to suppress the flow separation which occurs without control between the shock foot and the trailing edge and which is at the origin of the buffet phenomenon.

1 INTRODUCTION

In transonic flow conditions, the shock wave/boundary layer interaction induces a flow separation on the suction side of the wing which depending on the aircraft's Mach number and angle-of-attack can induce a flow instability called "buffet" and then structural vibrations called "buffeting". This flow instability consists in a shock location oscillation which results in a lift and drag oscillation. Buffeting can greatly affect aerodynamic behaviour. This is the reason why the buffeting phenomenon limits the aircraft's flight envelope. Since the separation is at the origin of the buffet, the objective of this study is to postpone the buffet onset by suppressing or decreasing the separation size by means of control devices. Two control means have been investigated: one passive (mechanical vortex generators (mech. VGs)) and one active (fluidic vortex generators). Previous studies done at ONERA ([1] [3]) have shown that mechanical VGs are able to delay the buffet onset to higher angles of attack. However, even if they have demonstrated their efficiency for buffet onset delay, mechanical vortex generators have the drawback to increase drag in nominal cruise conditions. This is the reason why fluidic VGs, which can be turned off, are also investigated. Moreover, they can be used in a closed-loop strategy to adapt the control to the flow and consequently to reduce mass-flux requirements which is an important constraint for aircraft manufacturers. In the framework of ONERA's internal research project BUFET'N Co [1], numerical simulations have been performed to define the geometry of the covert plate which have been mounted on a half-model. Then, this model has been tested in transonic conditions in the ONERA S3Ch wind tunnel.

There is a huge literature on control by mechanical VGs but very few have performed parametric studies on VG geometric characteristics like skew angle, spacing and even fewer for transonic flow. Among this literature on mechanical VGs, we can site the work done by Lin *et al.* [11] on the effect of the VGs height and Godard & Stanislas [12] on the effect of the skew angle, VGs height, length and spacing. In a previous ONERA's internal project [14], co-rotating rectangular vanes have been investigated to delay buffet onset. Their height was equal to the boundary layer thickness $h = \delta = 1$ mm. Their length was $l = 5h$ and their skew angle was $\beta = 30°$. They were located at $x/c = 33\%$ (mean shock location $x/c = 50\%$) which corresponds to $34h$ upstream of the shock. Three VGs spacing were studied: $\lambda = 10h$, $20h$ or $40h$ and it was found that $10h$ was the most effective to suppress separation.

Lin *et al.* [11] have used fluidic VGs for separation control over a ramp at low speed. They have found that the size of the streamwise vortices increases with the skew angle and that the optimum value was $\beta = 90°$. Godard & Stanislas [15] have performed, at low speed (10 $m.s^{-1}$) over a ramp without separation, a parametric study of the skew angle β (between 45° and 90°), the diameter d/δ (between 0.024 and 0.036), the spacing λ/d (between 6 and 16.7) and the velocity ratio VR (between 1.6 and 4.7). The pitch angle was fixed equal to 45°. They found that the optimal parameters were $\beta = 60°$ and $\lambda/d = 6$ and the skin friction increases with VR and d/δ. Scholz *et al.* [16] have studied the effect of the pitch and skew angle on a flat plate at $U_\infty = 15 m.s^{-1}$. The evolution of the momentum gain obtained with control as function of α and β shows that the optimum skew angle depends on the pitch angle: for $\alpha = 30°$, the optimum

value of β is 50° whereas for $\alpha = 45°$, the optimum value of β is lower and equal to 20°. This shows the necessity of optimizing both pitch and skew angles simultaneously and not separately. Rao [17] has performed an experimental study to control shock induced boundary layer separation with fluidic vortex generators. He has found that the optimum skew angle is 45°. Concerning the pitch angle, it should lie between 30° and 45°. Pearcey *et al.* [18] have performed experiments of shock-induced separation control by fluidic VGs for freestream Mach number between 1.25 and 1.65. They observed that only one streamwise vortices forms for a *VR* value which depends on the skew angle β and which is minimum for $\beta = 45°$. Two pitch angles α (30° and 45°) and three skew angles β (45° ; 60° ; 75°) have been investigated. The optimum angles found were $\alpha = 45°$ and $\beta = 60°$. Szwaba [19] have realized a genetic algorithm optimization of pitch and skew angles with Fluent. The freestream Mach number was $M_\infty = 1.25$. They found that the vorticity is maximum for $\alpha = 20°$ and $\beta = 70°$. Moreover, as observed by Scholz *et al.*, the optimum skew angle depends on the pitch angle value.

In this article, the work is limited to the study of mechanical VGs (skew angle, spacing and location) and continuous blowing fluidic VGs (pitch and skew angles) since the CPU time involved in the parametric study with a such large amount of parameters would have been far too large, even more so using 3D unsteady simulations.

This report is organized as follows. In section 2, the flow configuration (geometry, flow conditions) will be given. Then, in section 3, the numerical method (grid, turbulence model, VG modelling) will be presented. The results obtained with the mechanical and the fluidic VGs are gathered in section 4. Section 5 presents the first experimental results.

2 FLOW CONFIGURATION

2.1 Geometry

The geometry consists in the OAT15A-CA supercritical airfoil with a freestream chord length equal to the mean aerodynamic chord of the half-model that has been tested in the S3Ch wind tunnel (c = 0.22 m). The trailing-edge thickness is equal to 1% of the chord length and not 0.5% like in the OAT15A airfoil. The sweep angle is equal to 30°. The chord length taken normally to the leading edge is consequently equal to $c_n = 0.22 \times \cos(30°) = 0.1905$ m.

2.2 Flow conditions

The freestream conditions are a Mach number of $M_\infty = 0.843$ which gives a normal Mach number equal to 0.73. The chord-based Reynolds number Re_c is equal to 3.06×10^6, the stagnation pressure is equal to 1 bar and the stagnation temperature is equal to 300 K. Unless otherwise mentioned in the figures' captions, the angle-of attack in the freestream direction is equal to 3.5º which gives a normal-to-leading-edge angle-of-attack equal to $\tan^{-1}\left(\frac{\tan(3.5)}{\cos(30)}\right) = 4.04°$.

3 NUMERICAL METHOD

3.1 RANS modelling

The computational method used in this study relies on ONERA's structured, multiblock, cell-centered, *elsA* CFD software [4]. The Reynolds-averaged form of the Navier-Stokes equations is solved using Jameson's second order centred scheme with artificial viscosity for the spatial discretisation. The implicit phase is resolved using a LU-SSOR relaxation technique and convergence is accelerated through a one-level, v-cycle, multigrid algorithm. Two turbulence models have been used: the one-equation model of Spalart and Allmaras [5] and the two-equation k-ω SST of Menter [6]. Steady solutions were obtained using a quasi-stationary time-marching integration with a CFL-derived time-step. Since the CPU time involved in the parametric study with such a large amount of parameters and in 3D URANS would have been far too large, only 3D RANS computations have been performed.

To simplify mesh generation, the simulation of mechanical VGs does not use body conforming meshes but an alternative source term modelling (see [7] and [8] for more details), as proposed by Bender *et al.* [9]. Based on a lifting-line theory, it simply consists in adding a source term to the momentum components of the RANS equations.

3.2 Mesh

The mesh used for all the computations is shown in Figure 1. There are 476 cells around the airfoil with a refinement around the mean shock location and at the trailing-edge. The cell sizes in the three directions upstream of the shock are imposed following a previous study on the sensibility of VG model to the mesh size [10]. There are 25 cells in the streamwise direction around the marked cells, 49 cells in the wall-normal direction and 61 cells in the transverse direction. The mesh is composed of two parts: a 2D mesh in red (340,000 cells) and a 3D one in green (2.4 10^6 cells).

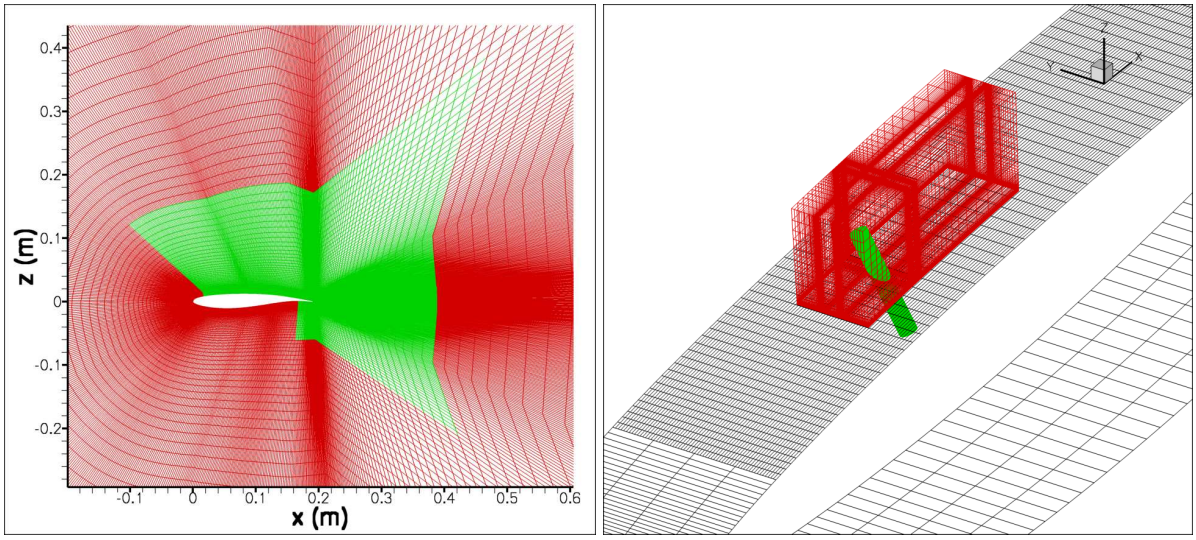

Figure 1 left: OAT15A mesh (red zone: 2D, green zone: 3D), right: close-up view around the fluidic VG mesh.

4 NUMERICAL SIMULATIONS

4.1 Mechanical vortex generators

Figure 2 presents an illustration showing the definition of mechanical VGs parameters for co-rotating and counter-rotating VGs. Since the model is swept, only co-rotating VGs have been investigated. Figure 2 (right) gives the definition of mechanical VGs skew angle β and spacing λ which are taken from the normal to the leading edge. To obtain the skew angle from the freestream direction, the sweep angle (30°) has to be added to the values of β given in the figures described below.

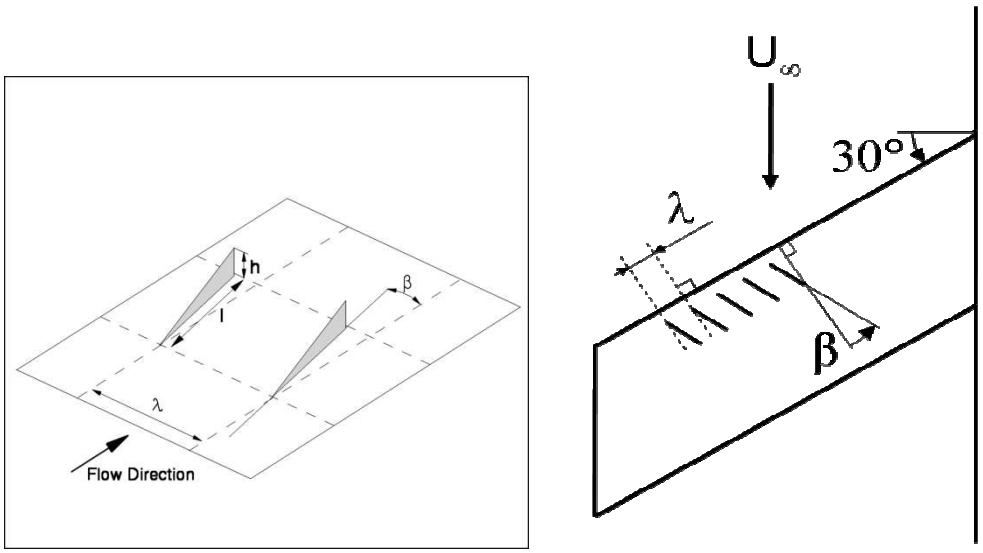

Figure 2 Sketch showing the different parameters defining the mechanical VGs shape for co-rotating VGs.

4.1.1 Skew angle and spanwise spacing effects

Because of the large number of variables describing the mechanical VGs geometry, some have been fixed based on previous parametric studies available in the literature [11] [12] [14]. The height of the VGs is equal to $h = \delta = 1.3$ mm, where δ is the boundary layer thickness. Their length is $l = 5h$. The effect of the VGs location on the suction side has also studied (not shown here for brevety). The results have shown that the optimum location was around 21% of chord. In this section, skew angle between $\beta = -70°$ and 20° have been investigated. Spanwise VGs spacing of $\lambda/h = 6$ and 10 have also been studied. Since the model is swept, only co-rotating VGs have been investigated.

An iso-surface of Q criterion coloured by the Mach number and an iso-surface $M = 1$ is shown in Figure 3. The mechanical VGs are located at $x/c = 21\%$ with a skew angle of 0°. This figure shows that the streamwise vortices created by the skewed vanes extend up to the shock foot. The separated zone downstream of the shock has been suppressed.

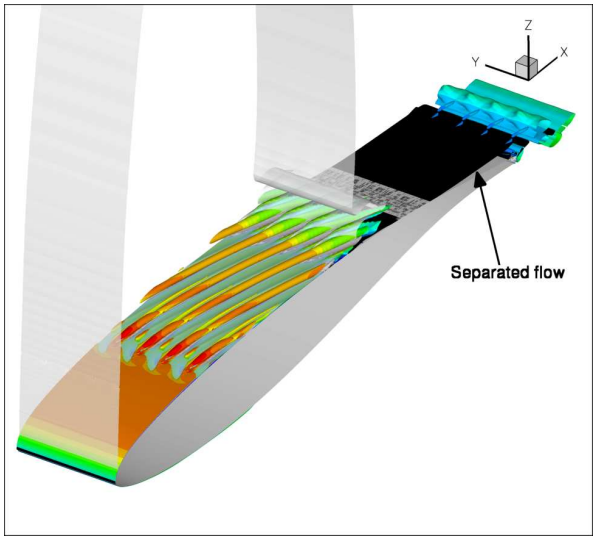

Figure 3 Q-criterion iso-surface ($Q = 100U_\infty^2 / h^2$) coloured by the Mach number and iso-surface M=1 showing the streamwise vortices created by the co-rotating mechanical VGs ($x/c = 21\%$, $\beta = 0°$, $\lambda/h = 6$).

The effect of VGs skew angle and spacing on lift and drag is shown in Figure 4 for VGs located at $x/c = 0.21$. The freestream directions corresponds to $\beta = -30°$. Symmetric skew angles with respect to the freestream direction have been studied: β varies between -70° (-40° with respect to the freestream direction) and 20° (50° with respect to the freestream direction). For $\beta = -70°$, -50° and -30°, the 3D RANS computation does not converge which means that the mechanical VGs are not able to suppress buffet. For the two spacing, the optimum skew angle lies between 0° (30° with respect to the freestream direction) and 10° (40° with respect to the freestream direction). If we look at the friction line directions, we can see that their skew angle is around 10° with respect to the freestream direction at the mechanical VGs location $x/c = 0.04$. The fact that the flow is swept can explained why the optimum skew angle values are slightly larger than the values found usually in the literature. Moreover, the effect of the skew angle is not symmetric with respect to the freestream direction. This can be explain by the fact that mechanical VGs with skew angles higher than -30° creates streamwise vortices with a vorticity with the same sign that the transverse boundary layer one. On the contrary, mechanical VGs with skew angles lower than -30° creates streamwise vortices with a vorticity with the opposite sign with respect to the transverse boundary layer one. So, their vorticity decreases rapidly as we will see in the following and they have no effect on lift. Figure 4 also shows that mechanical VGs with λ/h = 6 are more efficient that the ones with a larger spacing equal to $\lambda/h = 10$. This result is consistent with Godard & Stanislas [10] who also found that $\lambda/h = 6$ is the optimal spacing. Lower values of the spacing were found ineffective.

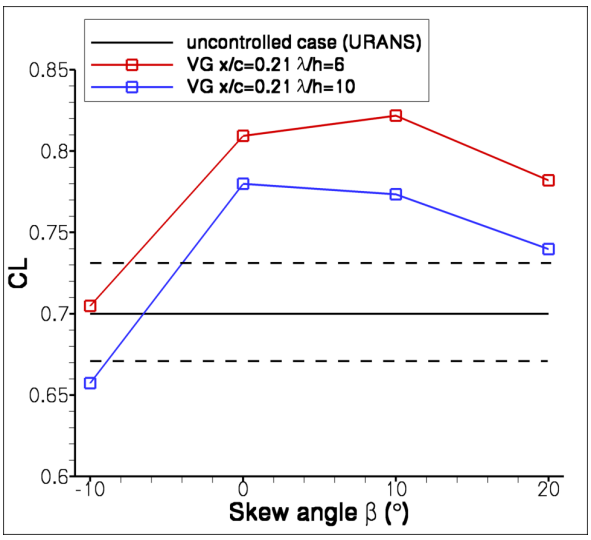

Figure 4 Lift evolution with the mechanical VGs skew angle β as defined in Figure 2 (horizontal dashed lines give the amplitude of the lift for the uncontrolled case computed in URANS).

The effect of the skew angle on the wall pressure distribution is shown in Figure 5 for VGs located at $x/c = 0.21$ and with a spacing $\lambda/h = 6$. Wall pressure distributions for skew angles lower than -10° are not since the 3D RANS computations do not converge. As expected from Figure 4, the higher the lift, the more downstream the shock.

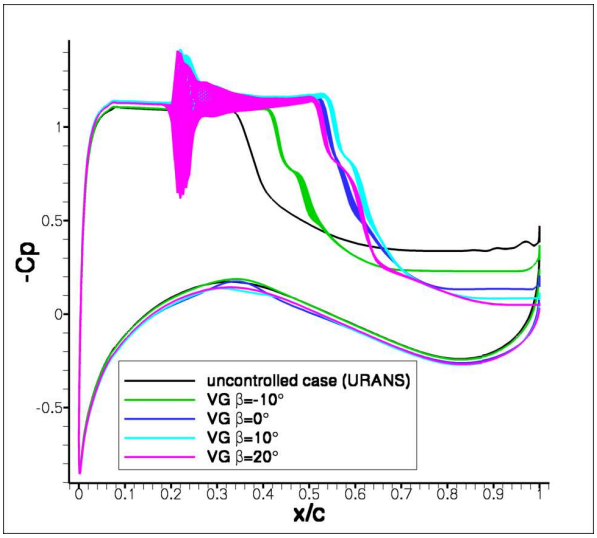

Figure 5 Wall pressure distribution for different mechanical VGs skew angles (x/c=0.21, λ/h=6).

4.2 Fluidic vortex generators

An illustration showing the definition of the geometric parameters describing co-rotating fluidic VGs is presented in Figure 6. It also shows the definition of the skew angle of the fluidic VGs (Figure 6 right).

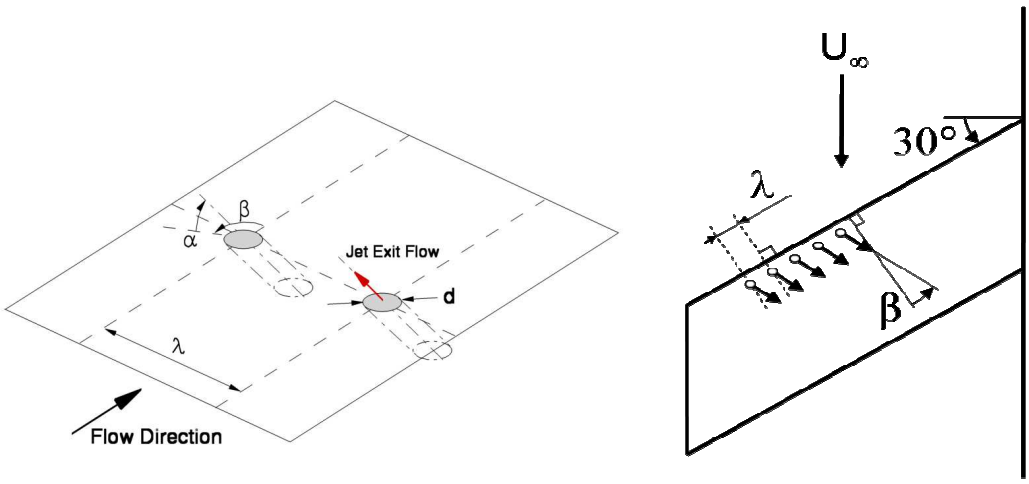

Figure 6 Sketch showing the different parameters defining the control with fluidic VGs.

4.2.1 Pitch and skew angles effects

The effects of pitch angle α and the skew angle β have been studied. The orifice is located at $x/c = 21\%$ which corresponds to the optimum location found for the mechanical VGs. The diameter d is chosen equal to the boundary layer thickness $\delta = 1.3$ mm and the spacing is equal to $10d$. The jet Mach number Mj is equal to 2 so the velocity ratio is 1.4. This Mach number is equal to the one of the ONERA's pulsed jet actuator. The momentum coefficient C_μ for one hole is defined by:

$$C_\mu = \frac{\rho_j S_j U_j^2}{\rho_l S U_l^2} \tag{1}$$

where ρ_j is the jet density, Sj the orifice surface based on the hole diameter (not the projected surface), Uj its velocity, ρ_l is the local crossflow density, S the airfoil surface for a span equal to $\lambda/h = 10$ and U_l is the local crossflow velocity. For jet Mach number equal to 2, the momentum coefficient C_μ is equal to $2\ 10^{-3}$ and the mass-flux per hole to 0.39 $g.s^{-1}$.
Figure 7 (left) shows the evolution of lift with the pitch angle α and the skew angle β. As observed by Scholz *et al.*, we can observe that the optimum skew angle depends on the pitch angle value: for $\alpha = 30°$, the optimum value of β is 60° whereas for $\alpha = 45°$, the optimum value of β is lower and equal to 20°. The optimum pitch and skew angles are $\alpha = 30°$ and $\beta = 60°$. If the skew angle is taken from the freestream direction, the optimum skew angle is equal to 90° (60° + sweep angle). This value is higher than what can be found in the literature ($\beta = 60°$) but in our case, the flow is swept.

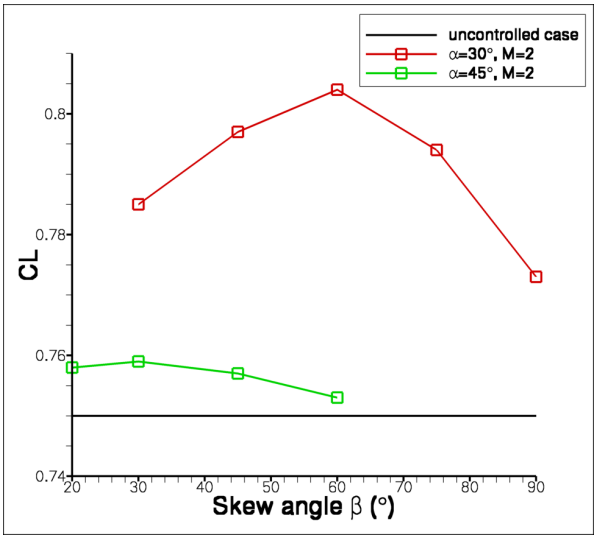

Figure 7 Lift evolution with the pitch angle α and the skew angle β for Mj = 2 (solid line: controlled case, dashed line: uncontrolled case).

5 EXPERIMENTAL RESULTS

Based on the previous numerical simulations, different cover plates with mechanical and fluidic VGs have been manufactured. Wind tunnel tests on a swept half-model have been performed in the S3Ch wind tunnel of the Fundamental and Experimental Aerodynamics Department of ONERA in Meudon. Figure 8 displays an oil flow visualisation of the uncontrolled flow for an angle-of-attack of 3.5º and a Mach number of $M_\infty = 0.82$. The green coloured oil comes from the pressure side of the wing whereas yellow coloured oil has been painted on the suction side. So, the green coloured zone on the suction side shows the extent of the separated zone. This separated zone extents from the shock foot up to the trailing edge on the outer wing.

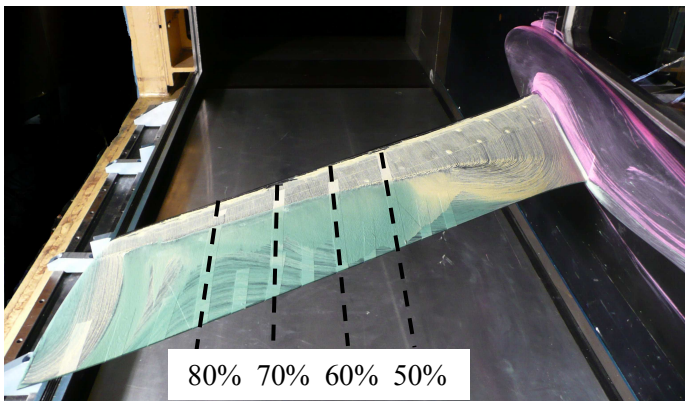

Figure 8 Oil flow visualisation of the uncontrolled flow ($\alpha = 3.5º$, $M_\infty = 0.82$).

Figure 9 shows an oil flow visualisation of the controlled flow with mechanical VGs for the same aerodynamic conditions. The flow separation has been suppressed except between 20 and 60% of the span where there remains a green oil zone. This is due to the fact that the flow is controlled only between 50 and 90% of the span so the flow separates between 20 and 50% of the span. Figure 9 also displays interesting three-dimensional flow patterns at the shock foot showing that the streamwise vortices formed downstream of the VGs deforms the shock as observed in Figure 3 for the numerical simulations. Figure 10 shows the wall pressure distribution for the baseline and the controlled flow with mechanical VGs. As shown by the *Cp* value at the trailing edge, the flow separation which is at the origin of the buffet phenomenon has been suppressed for span between 50 and 80%. As observed in Figure 5 for numerical simulations, since the flow separation has been reduced, the shock location has been postponed downstream.

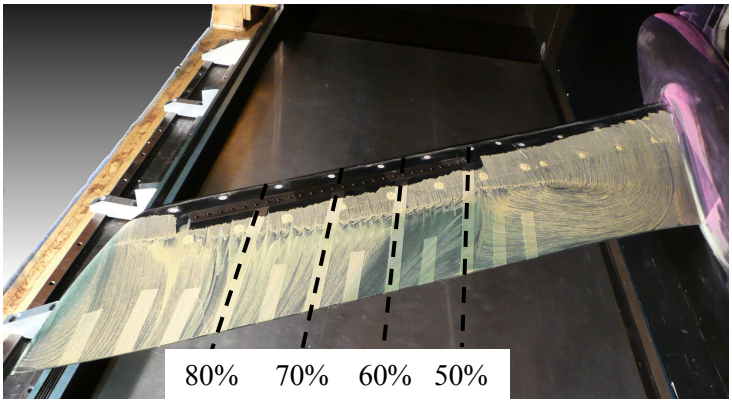

Figure 9 Oil flow visualisation of the controlled flow with mechanical VGs ($\alpha = 3.5º$, $M_\infty = 0.82$).

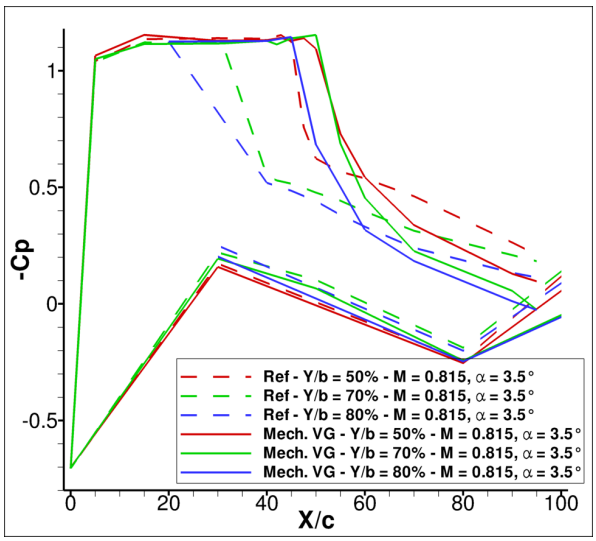

Figure 10 Wall pressure distribution of the controlled flow with mechanical VGs.

Figure 11 shows an oil flow visualisation of the controlled flow with fluidic VGs (α = 30°, β = 30°, Mj = 2) for the same aerodynamic conditions. The flow separation has been suppressed except between 50 and 60% of the span where there remains a small green oil zone. This figure shows that fluidic VGs are able to suppress separated zone in transonic conditions as mechanical VGs. Figure 12 shows as Figure 10 that the flow separation has been suppressed for span between 50 and 80%. The shock location has also been postponed downstream and the shock strength is larger. Figure 13 shows the wall pressure root-mean-square value distribution of the baseline, controlled flow with mechanical and fluidic VGs. It shows that the pressure fluctuations level downstream of the shock is lower in both controlled cases that in the uncontrolled case since the flow separation has been suppressed.

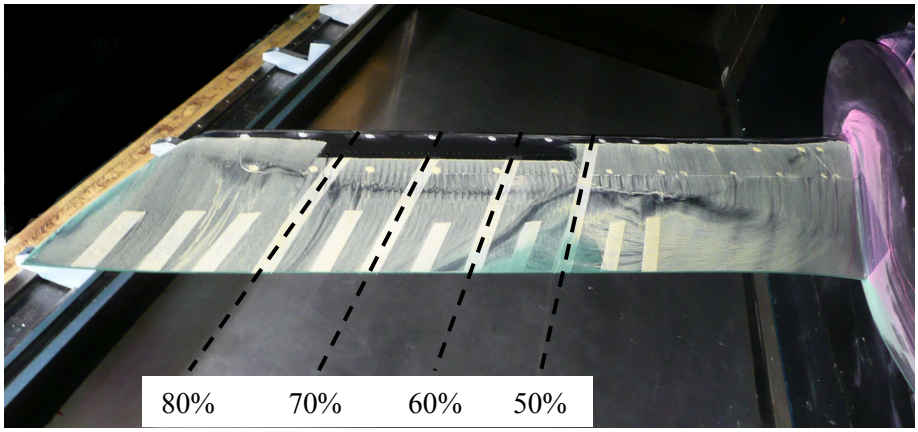

Figure 11 Oil flow visualisation of the controlled flow with fluidic VGs.

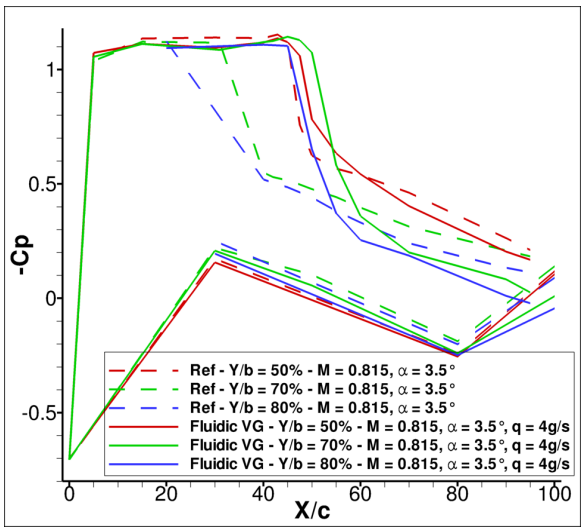

Figure 12 Wall pressure distribution of the controlled flow with fluidic VGs.

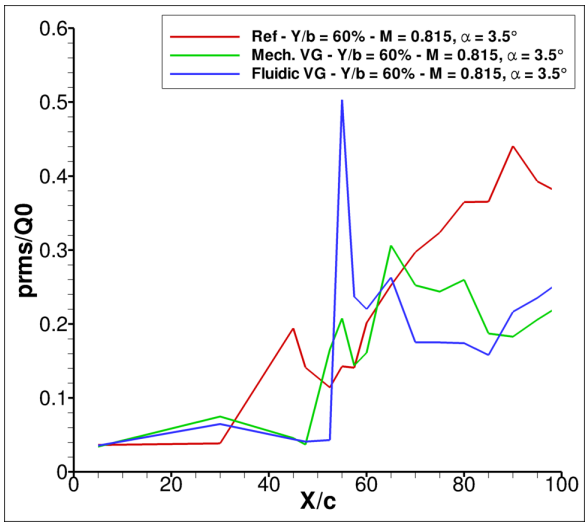

Figure 13 Wall pressure root-mean-square value distribution of the baseline, controlled flow with mechanical and fluidic VGs.

6 CONCLUSION

In the framework of ONERA's internal research project BUFET'N Co, numerical simulations have been performed to help in the choice of actuators parameters (actuator position, orifice diameter, pitch and skew angles…) for the design of the wing model's inserts which will be tested in the ONERA S3Ch wind tunnel at the beginning of the third year of the project. Three-dimensional RANS computations have been performed to study both passive (mechanical VGs) and active (fluidic VGs) actuators.

Concerning the mechanical VGs, three parameters have been studied: the location on the suction side, the skew angle and the spanwise spacing. The mechanical VGs height has been fixed equal to the local boundary layer thickness. The effect of those three parameters on the lift and wall pressure distribution has been investigated to determine the optimal parameters. To perform this study, the BAY model [7] [8] [9] implemented in *elsA* has been used. As observed by Godard & Stanislas [12], the optimal spacing is around $\lambda/h = 6$. Another point investigated is that, for swept model, the effect of the skew angle is not symmetric with respect to the freestream direction because mechanical VGs which create streamwise vortices with the opposite sign with respect to the transverse boundary layer see their vorticity decreases much faster that VGs which directions is pointed towards the wing root.

Concerning the fluidic VGs, two parameters have been studied: the pitch and skew angles. The jet Mach number is equal to 2. The spanwise spacing was fixed equal to $\lambda/d = 10$. The location was fixed at the optimum location found for the mechanical VGs ($x/h = 0.21$ for $\lambda/h = 10$) and the diameter was equal to the local boundary layer

thickness. In accordance with the literature, it has been found that the optimal skew angle depends on the pitch angle. For α = 30º, the optimal skew angle is β = 60º (as taken from the normal to the leading edge) where for α = 45º, the optimal skew angle is lower and equal to 30º. The optimal pitch and skew angles are α = 30º and β = 60º.

Then, the results of the numerical simulations were used to design inserts for a 3D half-model that has been in transonic conditions in the ONERA S3Ch wind tunnel. The experimental results have shown that both mechanical and fluidic VGs were able to suppress the massive flow separation which occurs without control between the shock foot and the trailing edge and which is at the origin of the buffet phenomenon. Pulsed fluidic VGs (not shown here) have also been tested and it has been shown that they were able to suppress separation as mechanical and continuous blowing fluidic VGs. The next step is now to compare the experimental data with three-dimensional numerical simulations of the half-model in the wind tunnel.

Acknowledgments

This work is being partly supported in the AVERT project for the numerical simulations, funded by the European Commission's Sixth Framework Programme (Project Contract No: AST5-CT-2006-030914) and by ONERA's own funding for wind tunnel tests.

References

1. E. Coustols, V. Brunet, D. Caruana, D. Sipp "BUFET´N Co: A Joint ONERA Research Project Devoted to Buffet Control on a Transonic 3D Wing Using Closed-Loop Approach", CEAS/KATnet II Conference on "Key Aerodynamic Technologies", 12-14 May 2009, Bremen, Germany.
2. D. Caruana, A. Mignosi, C. Robitaille and M. Correge "Separated flow and buffeting control", Flow, Turbulence and Combustion, Vol. 71, pp. 221-245, 2003.
3. V. Brunet "Numerical investigation of buffet phenomenon with URANS equation", 1st European Conference for Aerospace Sciences (EUCASS), Moscow, Russia, July 4-7, 2005.
4. L. Cambier and M. Gazaix "elsA: an efficient object-oriented solution to CFD complexity", AIAA Paper 2002-0108, 40th AIAA Aerospace Sciences Meeting & Exhibit, Reno, Nevada, January 14-17, 2002.
5. P. Spalart and S. Allmaras "A one-equation turbulence model for aerodynamic flows", La Recherche Aerospatiale, pp. 5-21, 1994.
6. F.R. Menter "Two-equation eddy-viscosity turbulence model for engineering applications", AIAA Journal, Vol. 32, No. 8, pp. 1598-1605, 1994.
7. V. Brunet, C. François, E. Garnier, M. Pruvost "Experimental and numerical investigations of vortex generators effects", 3rd AIAA Flow Control Conference, San Francisco (USA), June 5-8, 2006.
8. M. Meunier and V. Brunet "High-lift devices performance enhancement using flow control strategies", 7th ONERA-DLR Aerospace Symposium (ODAS), Toulouse (France), October 4-6, 2006.
9. E.E. Bender, B.H. Anderson, P.J. Yagle "Vortex generator modelling for Navier-Stokes codes", FEDSM 99-6919, July 1999.
10. N. De Cacqueray "Etude numérique de générateurs de tourbillons pour le contrôle d'écoulement", Stage de fin d'étude, Ecole Centrale de Lyon, 2007.
11. J.C. Lin "Exploratory study of vortex-generating devices for turbulent flow separation control", AIAA 91-0042, 29th Aerospace Sciences Meeting, Reno, NV, January 7-10, 1991.
12. G. Godard, M. Stanislas "Control of a decelerating boundary layer. Part 1: Optimization of passive vortex generators", Aerospace Science and Technology, vol. 10, pp. 181–191, 2006.
13. T. P. Bray "A parametric study of vane and air-jet vortex generators", PhD Thesis, Cranfield University, October 1998.
14. D. Caruana "Contrôle des décollements et du tremblement à l'aide d'actionneurs de type "générateurs de tourbillons". Ecoulement transsonique bidimensionnel", RT 2/06131 DMAE, Septembre 2002.
15. G. Godard, M. Stanislas "Control of a decelerating boundary layer. Part 3: Optimization of round jets vortex generators", Aerospace Science and Technology, vol. 10, pp. 455–464, 2006.
16. P. Scholz, J. Ortmanns, C.J. Kähler and R. Radespiel "Performance optimization of jet actuator arrays for active flow control", CEAS/KATnet Conference on Key Aerodynamic Technologies, Bremen, 20-22 June 2005.
17. M.K. Rao "An experimental investigation of the use of air jet vortex generators to control shock induced boundary layer separation", PhD thesis, City University, September 1988.
18. H.H. Pearcey, K. Rao, and D.M. Sykes "Inclined air-jets used as vortex generators to suppress shock-induced separation", Paper No. 40 in AGARD CP-534, Fluid Dynamics Panel Symposium on Computational and Experimental Assessment of Jets in Crossflow, Winchester, UK, April 1993.
19. R. Szwaba, P. Flaszynski, J. Szumbski and J. Telega "Shock wave – boundary layer interaction control by air-jet streamwise vortices", Proceedings of the 8th International Symposium on External and Computational Aerothermodynamics of Internal Flows, Lyon, 2-5 July 2007.